Volume 13, Issue 1, Page 88-97, 2024 https://doi.org/10.46810/tdfd.1423852 Research Article

BİNGÖL UNIVERSITY

Türk Doğa ve Fen Dergisi
Turkish Journal of Nature and Science
www.dergipark.gov.tr/tdfd

PSO Training Neural Network MPPT with CUK Converter Topology for Stand-Alone PV Systems Under Varying Load and Climatic Conditions

Mehmet YILMAZ[1], M. Fatih ÇORAPSIZ[1*]

[1] Ataturk University, Engineering Faculty, Electrical-Electronics Engineering, Erzurum, Türkiye
Mehmet YILMAZ ORCID No: 0000-0001-7624-4245
M. Fatih ÇORAPSIZ ORCID No: 0000-0001-5692-8367

**Corresponding author: corapsiz@atauni.edu.tr*

(Received: 22.01.2024, Accepted: 01.03.2024, Online Publication: 29.03.2024)

Keywords
Maximum power point tracking,
Particle swarm optimization based neural network,
CUK converter,
Boost converter

Abstract: Temperature and irradiance levels are two examples of environmental variables that affect the power value produced by photovoltaic panels. Therefore, in order to transfer the maximum power value from the PV panel to the load under varying climatic conditions, maximum power point tracking (MPPT) algorithms and DC-DC converter topologies are used. In this study, the performances of boost converter and CUK converter circuit topologies are investigated under variable irradiance and variable load conditions by using a neural network-based MPPT algorithm learning particle swarm optimization (PSO). As the first scenario, it is analyzed assuming that the temperature and irradiance values coming to the panel are constant. As the second scenario, the performance evaluation of the converter topologies according to the current, voltage and power parameters is made for the variable load situation. As the last scenario, the difference in the irradiance value coming to the panel depending on the sun's condition during the day has been examined. Canadian Solar CS6P-250P PV panel is used in the study. 50 kHz is selected as the switching frequency. According to the results obtained, it has been observed that the CUK converter circuit topology reaches the maximum power point faster than the boost converter circuit topology both in dynamic environmental conditions and load change, and the oscillation at this point is less. It is aimed to increase the performance of this method, which uses boost converter topology and MPPT in the literature, by applying CUK converter topology.

Değişken Yük ve İklim Koşulları Altında Müstakil Çalışan PV Sistemleri için CUK Dönüştürücü Topolojili PSO Eğitimli Sinir Ağı Tabanlı MPPT

Anahtar Kelimeler
Maksimum güç noktası takibi,
Parçacık sürü optimizasyon tabanlı sinir ağı,
CUK dönüştürücü,
Yükselten tip dönüştürücü

Öz: PV panellerden elde edilen güç değeri sıcaklık ve ışınım değerleri gibi çevresel faktörlere bağlı olarak değişmektedir. Bu nedenle değişen iklim koşullarında PV panelden maksimum güç değerinin yüke aktarılması için maksimum güç noktası izleme (MPPT) algoritmaları ve DC-DC dönüştürücü topolojileri kullanılmaktadır. Bu çalışmada, parçacık sürü optimizasyonu (PSO) öğrenen sinir ağı tabanlı MPPT algoritması kullanılarak, yükselten tip dönüştürücü ve CUK dönüştürücü devre topolojilerinin performansları değişken ışınım ve değişken yük koşulları altında incelenmiştir. İlk senaryo olarak panele gelen sıcaklık ve ışınım değerlerinin sabit olduğu varsayılarak analiz edilmiştir. İkinci senaryo olarak değişken yük durumu için akım, gerilim ve güç parametrelerine göre dönüştürücü topolojilerinin performans değerlendirmesi yapılmıştır. Son senaryo olarak ise gün içerisinde güneşin durumuna bağlı olarak panele gelen ışınım değerindeki farklılık incelenmiştir. Çalışmada Canadian Solar CS6P-250P PV panel kullanılmıştır. Anahtarlama frekansı olarak 50 kHz seçilmiştir. Elde edilen sonuçlara göre CUK dönüştürücü devre topolojisinin hem dinamik çevre koşullarında hem de yük değişiminde yükselten tip dönüştürücü devre topolojisine göre maksimum güç noktasına daha hızlı ulaştığı ve bu noktadaki salınımın daha az olduğu görülmüştür. Literatürde yükselten tip dönüştürücü topolojisi ve MPPT kullanan bu yöntemin performansının CUK dönüştürücü topolojisi uygulanarak arttırılması hedeflenmiştir.

1. INTRODUCTION

Due to factors such as technological developments, increasing population and developing industry, the need for electrical energy is increasing over time. Fossil energy fuels, which are used to meet the energy needs, that are of primary importance in the development of countries, are gradually depleted. The use of fossil energy fuels is decreasing day by day due to the harmful gases they emit to the environment. Renewable energy sources have been used in order to meet the increasing energy demand in recent years. The most important advantages of these resources are that they are clean, constantly renewable, reduce environmental pollution and have low operating costs. The most important renewable energy sources used today are hydroelectric energy, wind energy, solar energy, geothermal energy and wave energy. Solar energy systems are preferred because they have no fuel costs, contain no moving parts, are resistant to climate changes and directly convert solar energy into electrical energy. Photovoltaic (PV) panels are the most important part of solar energy systems. PV panels are obtained from the combination of PV cells. PV panels are connected in series or parallel to create an energy system at the desired power level. Another important factor affecting the PV panel efficiency is the amount of solar irradiance reaching to the panel. During the day, the amount of irradiance reaching to the panel is reduced in cases such as cloudy weather and tree shadows. As a result, the amount of power produced decreases and the panel efficiency decreases. For these reasons, MPPT algorithms are used to increase panel efficiency. MPPT algorithms basically try to provide maximum energy to the load by optimizing the duty ratio of the DC-DC converters that provide the connection between the PV panel and the load. MPPT control algorithms are divided into two groups as analog and digital control. MPPT is provided with the help of conventional controllers by comparing the reference voltage and output voltage produced PV panel in analog control. In the digital control method, the control signal is produced directly by the pulse width modulation (PWM) generator.

In both control methods, the aim is to transfer the power obtained from the PV panel to the load with the highest possible efficiency through optimization algorithms. Optimization algorithms are classified as classical and metaheuristic. Classical optimization algorithms are frequently preferred in real-time applications due to their advantages such as simple structure and easy applicability. The most used optimization algorithms for MPPT applications are perturb and observe algorithm (P&O) [1-8], incremental conductance algorithm (INC) [9]. MPPT is preferred as analog control method in fuzzy logic-based algorithms (FLC) [3,10-11], neural network-based (NN) [12-16] and machine learning based [17] algorithms. Under partial shading conditions, bypass diodes cause multiple local maximum points in the P-V characteristic. In this case, classical optimization algorithms cannot reach the global maximum because they follow the local maximum. Metaheuristic optimization algorithms are used to increase PV panel efficiency. Major metaheuristic optimization algorithms; African vulture optimization algorithm (AVOA) [18], crow search algorithm (CSA) [19], butterfly optimization algorithm (BOA) [20], whale optimization algorithm (WOA) [21], most valuable player algorithm (MVPA) [22], squirrel search algorithm (SSA) [23], shuffled frog-leaping algorithm (SFLA) [24,25], BAT search [26], Harris hawk optimization (HHO) [27], search and rescue algorithm (SRA) [28] and particle swarm optimization (PSO) [7,29-33]. There are comparisons of some metaheuristic optimization algorithms based on performance parameters such as complexity, efficiency, and convergence time [34,35]. Al-Majidi et al designed a feedforward artificial neural network (ANN) for MPPT. In order to increase the accuracy of the model designed for MPPT, the PSO algorithm is used for the initial weights and selection of the best topology. While training, irradiance values and temperature values are determined as input variables, and power value is determined as output variable. In order to prove the accuracy of the designed model, a real-time data collection system is created. With this system, 48500 data are collected in a year on sunny and cloudy days. The suggested approach is compared with P&O, FLC, and traditional ANN algorithms. The outcomes gained show that the proposed strategy is successful. A boost converter topology is recommended to raise the input voltage produced by the PV panel [36]. In this study, it is aimed to increase the performance of the proposed method by applying it to amplifying type and CUK converter circuit topologies. This paper is structured as follows: PV cell model, boost converter, CUK converter, PSO, NN and PSO training NN are explained in Sect. 2. The simulation model created to compare the performance of the boost converter and CUK converter circuit topologies and the results are presented comparatively in Sect. 3. Finally, conclusions are given is Sect. 4.

2. MATERIAL AND METHOD

2.1. PV Cell Model

PV cells are obtained from the combination of p-n semiconductor elements. PV cells are semiconductor materials that generate current depending on the irradiance value. The most frequently used single-diode PV cell model in the literature for modeling PV cells is shown in Figure 1 [37]. I_{pv} is the current produced by light photons, I_d is the diode current, G is the irradiance value from the sun, T is the temperature value, V_P is the voltage value obtained from the PV panel. In materials with a thin film structure made up of extremely thin layers, R_p represents the total of the resistances formed between the layers and surrounding the cell, and R_s represents the sum of the resistances of the semiconductor material forming the cell and the contact resistances formed at the junction points of the cells.

Nomenclature	Abbreviation		
PV	Photovoltaic	BOA	Butterfly optimization algorithm
MPPT	Maximum power point tracking	WOA	Whale optimization algorithm
PWM	Pulse width modulation	MVPA	Most valuable player algorithm
P&O	Perturb and observe	SSA	Squirrel search algorithm
FL	Fuzzy logic	SFLA	Shuffled frog-leaping algorithm
P&O	Perturb and observe	HHO	Harris hawk optimization
INC	Incremental Conductance	SRA	Search and rescue algorithm
NN	Neural networks	PSO	Particle swarm optimization
CSA	Cuckoo search algorithm	ANN	Artificial neural network
BLDC	Brushless direct current	ML	Machine Learning
AVOA	African vulture optimization algorithm		

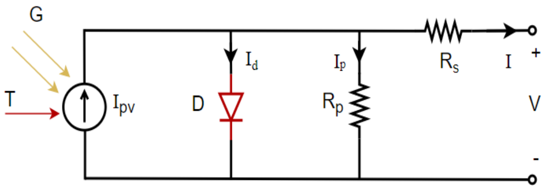

Figure 1. Single diode PV cell model [16]

The equations for modeling PV panels are given in Equations (1-5).

$$I = I_{pv} - I_d - I_p \tag{1}$$

$$I_d = I_0\left(e^{\frac{qV_d}{kT}} - 1\right) \tag{2}$$

$$V_d = V + IR_S \tag{3}$$

$$I_d = I_0\left(e^{\frac{q(V+IR_S)}{nkT}}\right) \tag{4}$$

$$I = I_{pv} - I_0\left(e^{\frac{q(V+IR_S)}{nkT}}\right) - \frac{V + IR_S}{R_p} \tag{5}$$

Where n represents the diode ideality constant, T represent for the cell temperature (K), k is the Boltzman constant (J/K), q is the electron charge (C) and I_0 represents reserve saturation current (A). Canadian Solar CS6P-250P was used as PV panel in the study. The features of this panel are given in Table 1.

Table 1. Canadian Solar CS6P-250P

Parameters	Value
Maximum Power	*249.83 W*
Open Circuit Voltage	*37.2 V*
Vmp	*30.1 V*
Isc	*8.87 A*
Imp	*8.3 A*
Temperature coefficient of Isc (%/deg.C)	*0.063698*
Temperature coefficient of Voc (%/deg.C)	*-0.3654*
Ncell	*60*

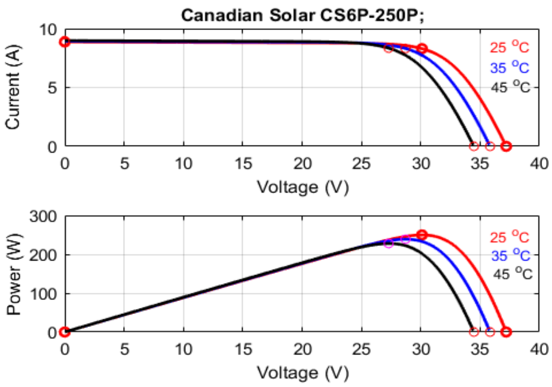

Figure 2. PV system curves at fixed 1000 W/m2 irradiance value

The two most significant factors influencing PV panel output power are temperature and irradiance levels. Figure 2 shows the voltage dependent variation of the output power and current of the Canadian Solar CS6P-250P PV panel according to the constant irradiance and variable temperature values. It is seen that as the temperature value increases, the voltage value decreases and the power value increases in Figure 2.

Figure 3 illustrates the variation of the output power and current depending on the voltage, according to the constant temperature and variable irradiance values. As can be seen from Figure 3, the current value decreases as the irradiance value decreases. In addition, since the power value depends on the voltage and current values, it is seen that there is a decrease in this value.

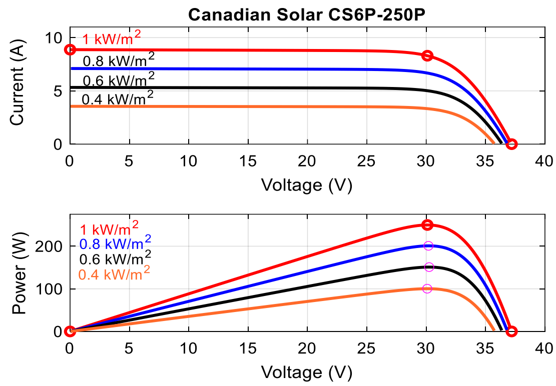

Figure 3. PV system curves at fixed 25̊C temperature value

2.2. Boost Converter Model

Step up circuit topologies that transfer the unadjusted DC voltage value applied to the input to the output at higher levels and adjustable. It is also known as step up converter. It operates in two different states depending on the open or close state of the switching element. In the case of switching is ON-mode, the diode is polarized in the opposite direction and shows open circuit property. In the case of switching is OFF-mode, the diode is forward-biased and shows short-circuit characteristics. The boost converter circuit topology is shown in Figure 4 [16].

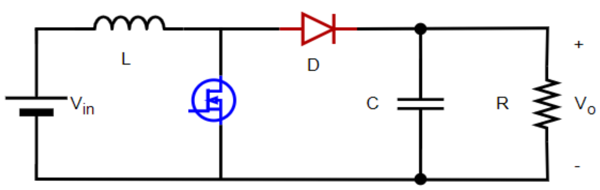

Figure 4. Boost converter circuit topology

The boost converter parameters are determined using the following equations. Average output current;

$$I_0 = \frac{P}{V_0} \tag{6}$$

$$\Delta I = (0.05)\frac{I_0\, V_0}{V_{in}} \tag{7}$$

$$\Delta V = V_0(0.01) \tag{8}$$

Inductance;

$$L = \frac{V_{in}\,(V_0 - V_{in})}{f \Delta I V_0} \tag{9}$$

Capacitance;

$$C = \frac{V_{in}\,(V_0 - V_{in})}{f \Delta I V_0} \tag{10}$$

The circuit parameters of the boost converter used in simulation studies are given in Table 2.

Table 2. The parameters of Boost converter topology

Parameters	Value
L	*1 mH*
C_{in} and C_2	*100 µF- 42.5 µF*
R_L	*30 Ω*
Switching Frequency (f)	*50 kHz*

2.3. CUK Converter Model

CUK circuit topologies that transfer the DC voltage value applied to the input to the output at higher or lower levels. Today, CUK converters are used in brushless direct current (BLDC) motor driver circuits, renewable energy systems and pulse width modulation (PWM) based PV systems. The most important difference of CUK converters from other converters is the use of capacitors for energy transfer. The CUK converter circuit topology is shown in Figure 5.

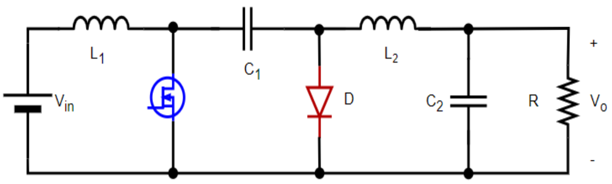

Figure 5. CUK converter circuit topology

The following equations are used in the CUK converter design given in Figure 5;

Duty ratio;

$$D = -\frac{V_0}{V_{in} - V_0} \tag{11}$$

Average inductance currents;

$$i_{L1} = \frac{P_s}{V_{in}} \tag{12}$$

$$i_{L2} = \frac{P_s}{-V_0} \tag{13}$$

Rate of change inductance currents;

$$\Delta i_{L1} = i_{L1}(\%10) \tag{14}$$

$$\Delta i_{L2} = i_{L2}(\%10) \tag{15}$$

Inductances;

$$L_1 = \frac{V_{in}\, D}{f \Delta i_{L1}} \tag{16}$$

$$L_2 = \frac{V_{in}\, D}{f \Delta i_{L2}} \tag{17}$$

Rate of change capacitance voltage;

$$\Delta V_{c1} = (V_{in} - V_0)\, 0.01 \tag{18}$$

Load resistance;

$$R = \frac{{V_0}^2}{P} \tag{19}$$

Capacitances;

$$C_1 = \frac{V_0\, D}{R f \Delta V_{c1}} \tag{20}$$

$$C_2 = \frac{1 - D}{0.01 f^2 8 L_2} \tag{21}$$

where we have; V_{in} input voltage (V), V_0 output voltage (V), i_L average inductance current (A), D duty ratio, Δi_L rate of change inductor current, L inductance (H), C capacitance (F), ΔV_c rate of change capacitor voltage, R load resistance (Ω), f switching frequency (Hz), r ripple, r_{c1} ripple at C_1.

Circuit parameters of the CUK converter used in simulation studies are given in Table 3.

Table 3. The parameters of CUK converter

Component	Parameters
L_1 and L_2	*5.74 µH – 1.59 µH*
C_1 and C_2	*39.5 µF- 8.36 µF*
R_L	*30 Ω*
Switching Frequency	*50 kHz*

2.4. Particle Swarm Optimization

The PSO algorithm was first developed in 1995 by R.C. It was introduced by Eberhart and J. Kennedy. The basis of the algorithm is based on the behavior of flocks of birds. Swarms are made up of particles. Each particle adjusts its position to its best position, taking advantage of its previous experience. Afterwards, all particles update their position according to the best particle of the swarm. This process continues until the goal is reached. In Figure 6, the flow chart of the PSO algorithm is given. The particle velocity and position are shown in the equations below. The velocity and position information of the particles are calculated according to Equation 22 and Equation 23 [31].

$$v_{k+1}^i = w v_k^i + c_1 rand \frac{p^i - x_k^i}{\Delta t} + c_2 rand \frac{p_k^g - x_k^i}{\Delta t} \tag{22}$$

$$x_{k+1}^i = x_k^i + v_{k+1}^i \tag{23}$$

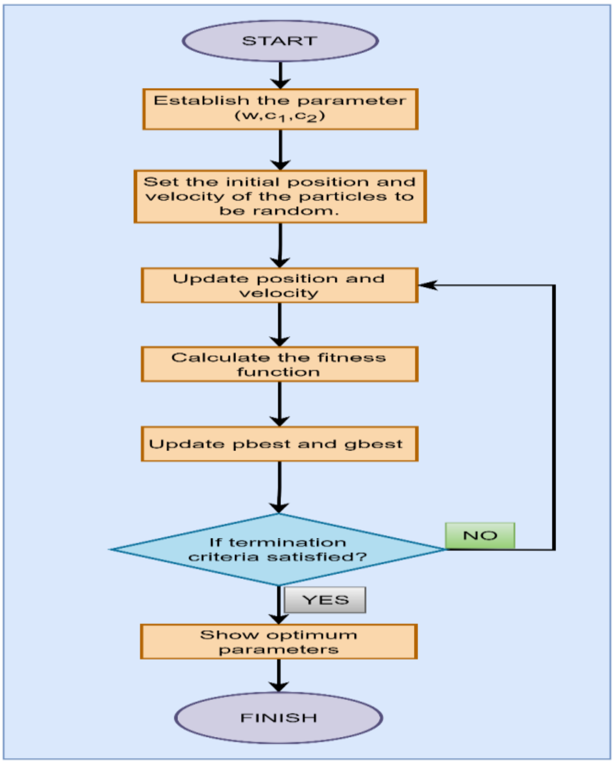

Figure 6. PSO flowchart

2.5. Neural-Network Model

The first artificial neural network model was created in 1943 by W. McCulloch and W. Pitts. In general, neural networks have usage areas such as system modeling, handwriting recognition, automatic vehicle control, voice recognition, fingerprint recognition and meteorological interpretation. An artificial neuron is shown in Figure 7.

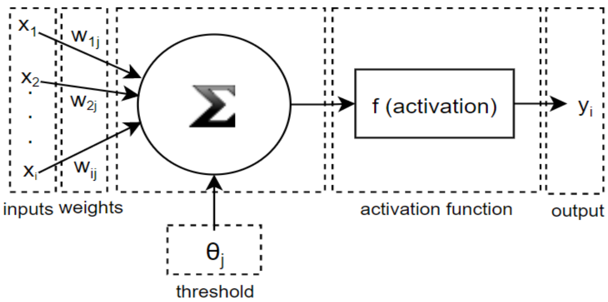

Figure 7. Artificial neuron

2.6. PSO training Neural-Network Model

PSO algorithm is used in training neural networks in order to obtain faster training process and convergence time. The algorithm is started by choosing a random location for each particle. The velocity and position information of each particle is updated using Equation 22 and Equation 23 by creating loops as many as the number of particles. Then the *Gbest* value is updated by comparing it with the *Pbest* values in each iteration. Finally, the algorithm is terminated by looking at the stopping criteria. The flowchart of NN training with PSO is shown in Figure 8.

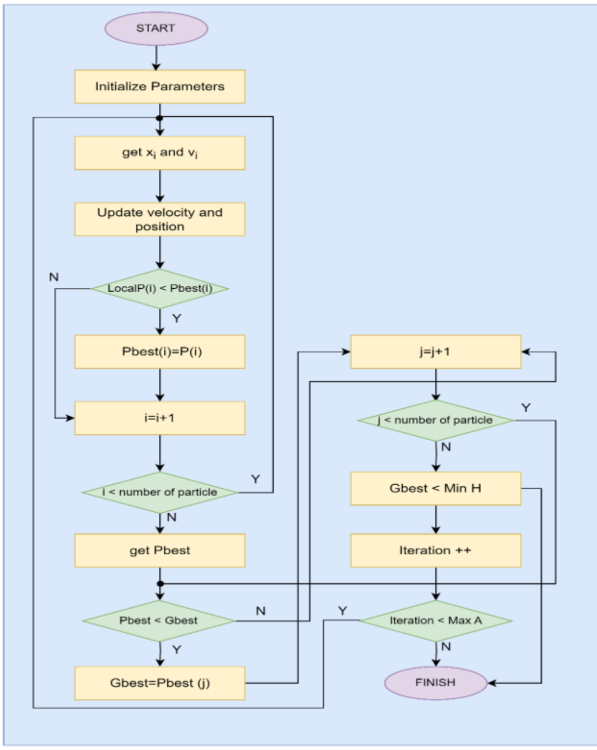

Figure 8. PSO training NN Algorithm [38]

3. RESULTS AND DISCUSSION

The simulation model shown in Figure 9 was created to compare the performances of the boost converter and the CUK converter. While creating the simulation model, Canadian Solar CS6P-250P was chosen as the PV panel. Boost converter and CUK converter circuit topologies are utilized as DC-DC converter architectures to raise the voltage at the panel output. *30Ω* resistive as load, PSO trained neural network maximum power point tracking (NN MPPT) algorithm is used to optimize the duty ratios of converter topologies. The irradiance values were determined as *1000 W/m²*, *800 W/m²*, *600 W/m²*, *400 W/m²* in the first case, constant *700 W/m²* in the second case and a *trapezoidal function* in the last case. Irradiance values for different scenarios are shown in Figure 10.

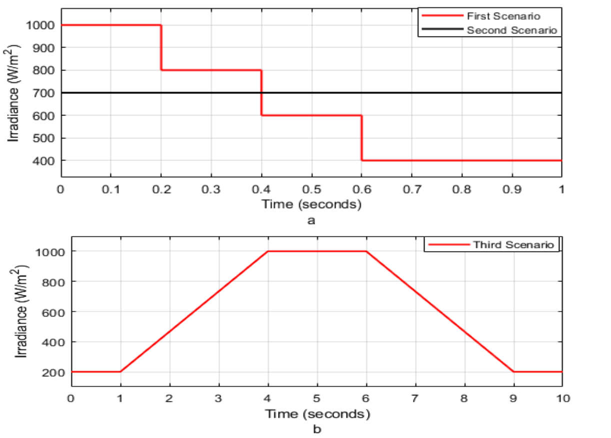

Figure 10. Irradiance values for a) first and second scenarios, b) third scenario

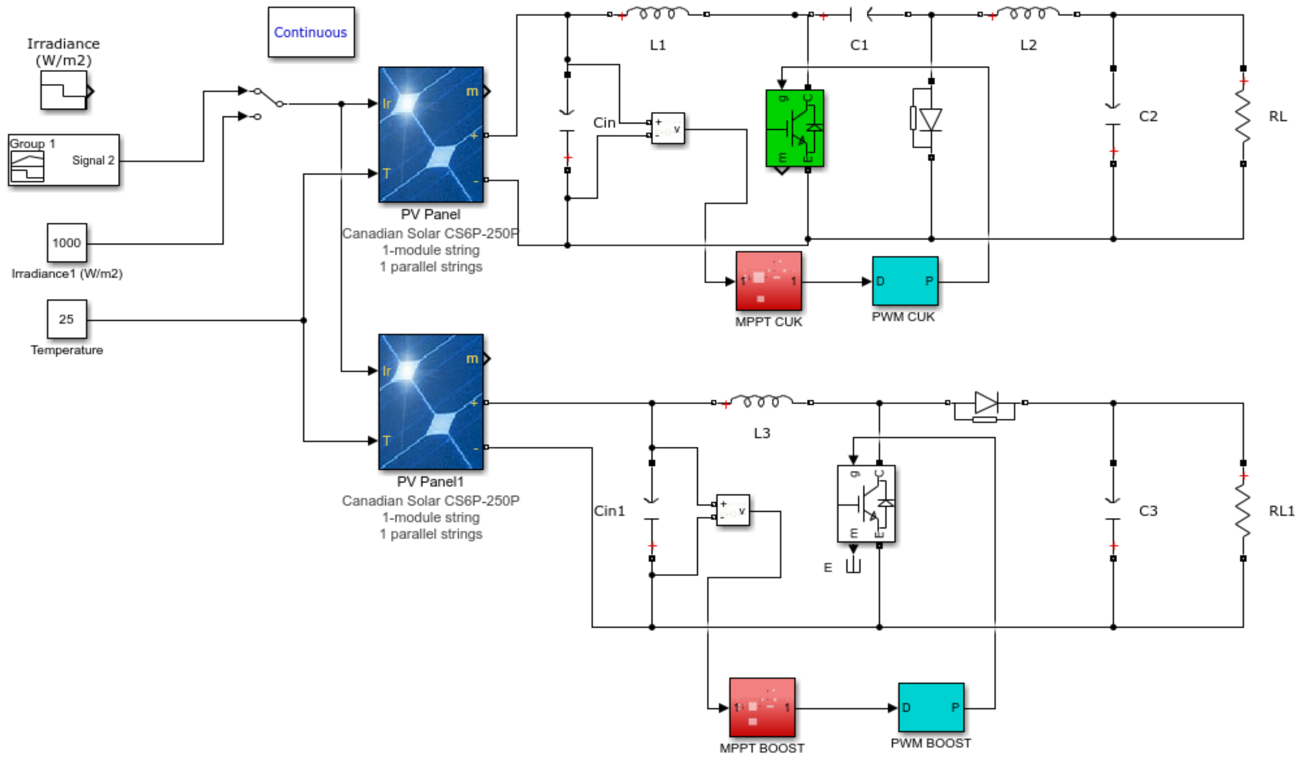

Figure 9. Simulation Model

First Scenario: In the first scenario, the irradiance value was initially selected as *1000 W/m²* and the converter performances were examined by reducing *200W/m²* in *0.2s* intervals. The irradiance value was determined as *800 W/m²* in the *0.2-0.4s* time interval, *600 W/m²* in the *0.4-0.6s* time interval and *400 W/m²* in the *0.6-0.9s* time interval. Irradiance values are chosen as high, medium and low irradiance levels and the changes in current, voltage and power at these values are investigated. The temperature was determined as *25°C* fixed values. Figure 11 shows the time-dependent variation of the load currents of the boost converter and CUK converter circuit topologies.

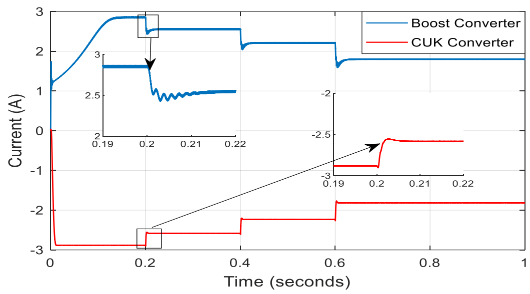

Figure 11. Boost converter and CUK converter output currents

In Table 4, the current values of both converters are given for the scenario determined above.

Table 4. The performance of Boost and CUK converter topologies

Time	Irradiance Value	Boost Converter	CUK Converter
0-0.2s	*1000 W/m²*	*2.856A*	*-2.88A*
0.2-0.4s	*800 W/m²*	*2.558A*	*-2.58A*
0.4-0.6s	*600 W/m²*	*2.21A*	*-2.24A*
0.6-1s	*400 W/m²*	*1.81A*	*-1.83A*

In Figure 12, the change in the voltage values of the boost converter topology and the CUK converter topology due to the decrease in the irradiance value at certain time intervals is shown.

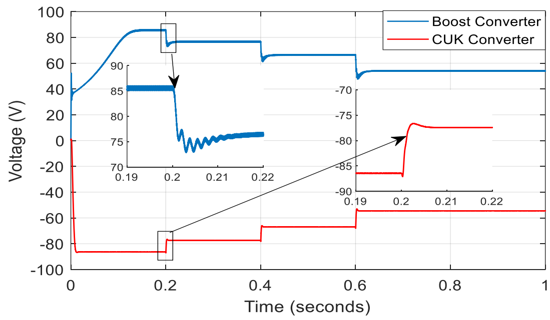

Figure 12. Boost converter and CUK converter output voltages

The variation of the load voltage obtained depending on the irradiance value with respect to time is given in Table 5.

Table 5. The performance of Boost and CUK converter topologies

Time	Irradiance Value	Boost Converter	CUK Converter
0-0.2s	*1000 W/m²*	*85.6V*	*-86.5V*
0.2-0.4s	*800 W/m²*	*76.6V*	*-77.5V*
0.4-0.6s	*600 W/m²*	*66.5V*	*-67V*
0.6-1s	*400 W/m²*	*54V*	*–54.5V*

In Figure 13, the variation of the power consumed on the load connected to the output in DC-DC converter topologies according to time is given.

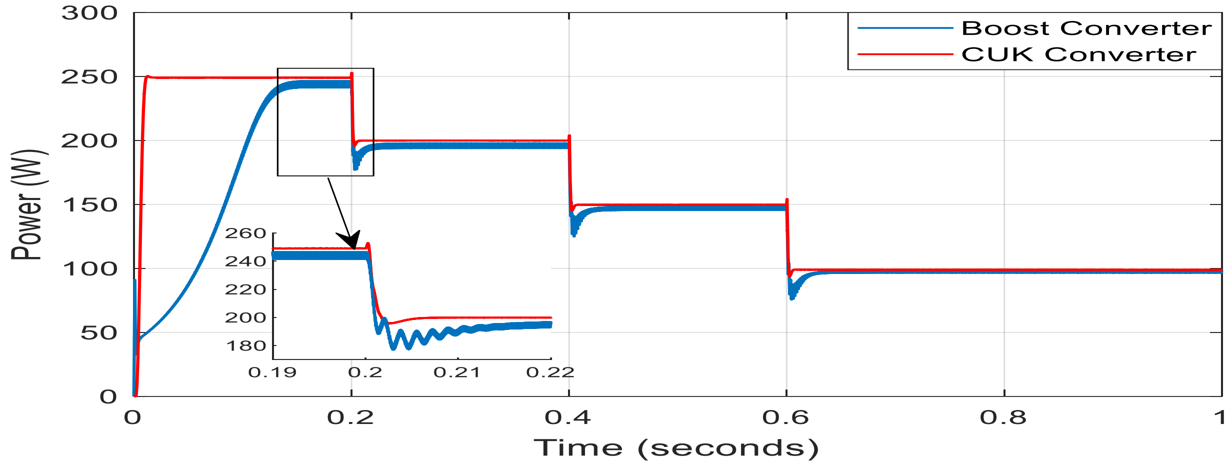

Figure 13. Boost converter and CUK converter output powers

In Table 6, the power values transferred to the load for the first scenario are shown in comparison.

Table 6. The performance of Boost and CUK converter topologies

Time	Irradiance Value	GMPP	Boost Converter	CUK Converter
0-0.2s	*1000 W/m²*	*249.83W*	*244.5W*	*249.12W*
0.2-0.4s	*800 W/m²*	*201.56W*	*196 W*	*200.5W*
0.4-0.6s	*600 W/m²*	*152.01W*	*147W*	*150.6W*
0.6-1s	*400 W/m²*	*101.36W*	*98W*	*99.5W*

When the results of both converters are examined, it is seen that the CUK converter circuit topology reaches the MPP point in a shorter time compared to the boost converter topology for the first scenario. In addition, it has been observed that there is less oscillation in the current, voltage and power values of the CUK converter circuit topology at the MPP point. The performance criteria such as settling time, rise time and oscillation (output power) of these two converters are shown in Table 7 comparatively.

Table 7. Comparison of Boost and CUK converter performance (0-0.2s)

Performance Metrics	Boost Converter		CUK Converter
Settling time (sec)	*132 ms*		*10 ms*
Rise time (sec)	*110 ms*		*5.14 ms*
Oscillation (%)(Power)	*% 1.78*		*% 0.22*

Second Scenario: In the second scenario, the effect of load change on converter performance (current, voltage and power) was examined by keeping the irradiance value and temperature constant. For this purpose, the irradiance value is determined as *700 W/m²* and the temperature was determined as *25°C* fixed values. The situation where the load value changes at intervals of *0.3s* has been examined. The load value was determined as *20Ω* in the *0-0.3s* time interval, the load value in the *0.3-0.6s* time interval as *25Ω* and the load value in the *0.6s* and later time period as 30Ω.

Figure 14 shows the variation of the currents of the boost converter and CUK converter circuit topologies for the load change situation at certain time intervals.

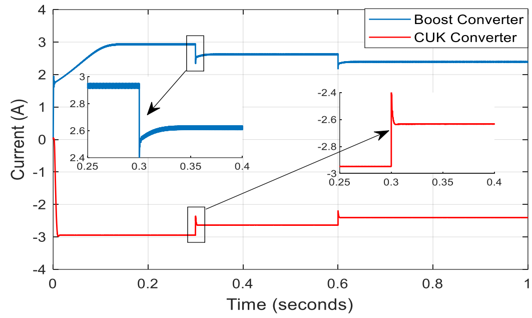

Figure 14. Boost converter and CUK converter output currents

As the load value connected to the output of the converter changes, the current value also changes accordingly. The current values obtained for this scenario are shown in Table 8.

Table 8. The performance of Boost and CUK converter topologies

Time	Irradiance Value	Load	Boost Converter	CUK Converter
0-0.3s	*700 W/m²*	*20Ω*	*2.98A*	*-2.95A*
0.3-0.6s	*700 W/m²*	*25Ω*	*2.62A*	*-2.63A*
0.6-1s	*700 W/m²*	*30Ω*	*2.39A*	*-2.4A*

Figure 15 shows the time-dependent variation of the output voltages of the second scenario boost converter and CUK converter.

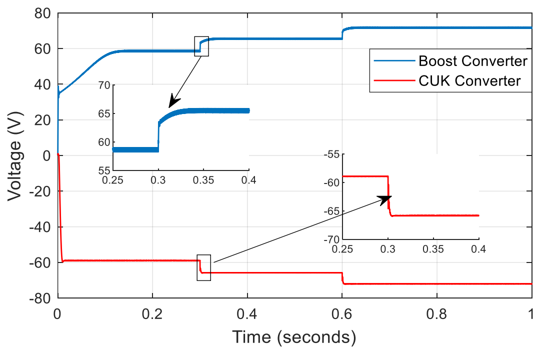

Figure 15. Boost converter and CUK converter output voltages

The change in the current value affects the voltage value so that the power transferred to the load remains constant. The output voltage values of both converters for *700 W/m2* fixed irradiance value and variable load values are given in Table 9.

Table 9. The performance of Boost and CUK converter topologies

Time	Irradiance Value	Load	Boost Converter	CUK Converter
0-0.3s	*700 W/m²*	*20Ω*	*58.6V*	*-59V*
0.3-0.6s	*700 W/m²*	*25Ω*	*65.5V*	*-65.8V*
0.6-1s	*700 W/m²*	*30Ω*	*71.8V*	*-72.1V*

Figure 16 is given for the type converter and the CUK converter topology that amplify the time-dependent variation of the power dissipated on the load.

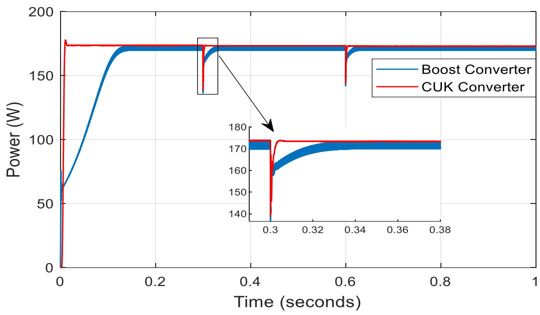

Figure 16. Boost converter and CUK converter output powers

In Table 10, the power values transferred to the load for the second scenario situation are presented.

Table 10. The performance of Boost and CUK converter topologies

Time	Irradiance Value	Load	GMPP	Boost Converter	CUK Converter
0-0.3s	*700 W/m²*	*20Ω*	*176.941 W*	*171.6W*	*174W*
0.3-0.6s	*700 W/m²*	*25Ω*	*176.941 W*	*171.6W*	*174W*
0.6-1s	*700 W/m²*	*30Ω*	*176.941 W*	*171.6W*	*174W*

It has been observed that the CUK converter circuit topology reaches the MPP point quickly for the situation where the load value changes at certain intervals, while the boost converter topology cannot fully reach the MPP point and oscillates more in current, voltage and power values. DC-DC converters performance parameters rise time, settling time and oscillation (%) for the two designed models are given in Table 11.

Table 11. Comparison of Boost and CUK converter performance (0-0.2s)

Performance Metrics	Boost Converter	CUK Converter
Settling time (sec)	*122 ms*	*9 ms*
Rise time (sec)	*90 ms*	*4.1 ms*
Oscillation (%)(Power)	*% 2.298*	*% 0.115*

Third Scenario: As the last scenario, the difference in the irradiance value coming to the panel depending on the sun's condition during the day has been examined. In order to evaluate this situation, a function whose irradiance value changes trapezoidal is chosen. The variation of irradiance with time for this scenario is shown in Figure 10b. At *700 W/m²*, 25 °C, GMPP is 50.027W, while for *1000 W/m²*, 25 °C, the GMPP is 249.83W. The boost converter output power is given in Figure 17.

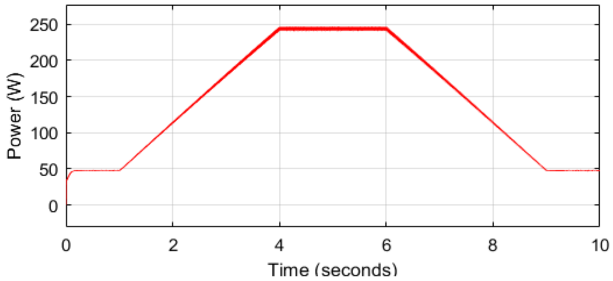

Figure 17. Boost converter output power

The irradiance value was determined as *200 W/m²* in the *0-1s* time interval. In this case, the settling time is *0.123s* and the output power is *47.5W*. In the *1-4s* time interval, the irradiance value increased linearly. Depending on the increase in irradiance, the power value transferred to the load also increased. In the case of *1000 W/m²* irradiance in the *4-6s* time interval, the power value is *244.5W*. While the irradiance decreases linearly between *6-9s*, the power value also decreases as the power value changes directly proportional to the irradiance. Finally, when the irradiance value is considered *200 W/m²* again, the output power value is measured as *47.5W*.

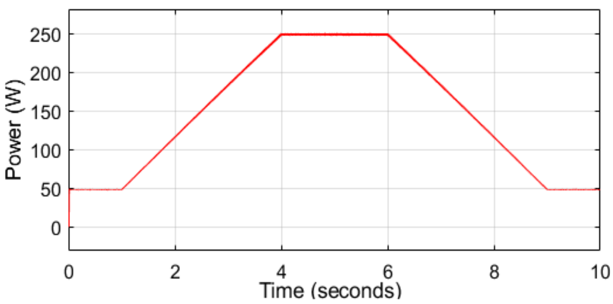

Figure 18. Boost converter output power

The CUK converter output power is seen in Figure 18. The output power value transferred to the load in the *0-1s* time interval was measured as *48W* in *0.016s*. Figure 18 shows an increasing power change in response to the increasing irradiance value in the *1-4s* time interval, and a decreasing power change depending on the decreasing irradiance value in the between *6-9s*. The power is 249.6W in the between *4-6s*. Finally, when the irradiance value is considered as *200 W/m²* again, the power value is measured as *48W*.

4. CONCLUSION

Solar energy systems are the most preferred renewable energy source due to their low maintenance costs. In order to adjust the output voltage of the PV panel to the desired values, booster type and CUK converter topologies are used. In this study, the PSO-based NN optimization algorithm was applied to both converter topologies. The performance of the converters for different scenarios was compared according to parameters such as settling time, rise time and oscillation. Firstly, DC-DC converter topologies for variable irradiance conditions are compared and performance criteria are presented. As the second scenario, the performance evaluation of the converter topologies according to the current, voltage and power parameters is made for the variable load situation.

In this situation, the CUK converter topology has reached its MPP by responding faster to all load change situations. Since the angle of incidence of the sun rays cannot reach the panels at the same rate during the day, the irradiance value is determined as a trapezoidal function in order to evaluate this scenario. The performance of the DC-DC converters under these scenarios is investigated. It is observed that the CUK converter responds faster to changes and reaches MPP earlier than the boost converter. In studies conducted for three different cases, it is observed that the CUK converter reaches the MPP faster and oscillates less than the boost converter. Matlab/Simulink program is used for simulation studies. PSO algorithm is frequently preferred in optimization problems due to its advantages such as simple structure and easy applicability. In this study, the panel data is trained with a neural network based on the PSO optimization algorithm. CUK converter circuit topology has been applied to this method, which is mostly used with boost converter structure in the literature, and it has been tried to contribute to the relevant field and successful results have been obtained. As a future research, the application of different optimization algorithms that have not yet been applied in this field to these systems will be studied.

REFERENCES

[1] Kamran M, Mudassar M, Fazal MR, Asghar MU, Bilal M, Asghar R. Implementation of improved Perturb & Observe MPPT technique with confined search space for standalone photovoltaic system. Journal of King Saud University-Engineering Sciences.2020; 32(7), 432-441.

[2] Pillai DS, Ram JP, Ghias AM, Mahmud MA, Rajasekar N. An accurate, shade detection-based hybrid maximum power point tracking approach for PV systems. IEEE Transactions on Power Electronics. 2019; 35(6), 6594-6608.

[3] Khan MJ, Pushparaj. A novel hybrid maximum power point tracking controller based on artificial intelligence for solar photovoltaic system under variable environmental conditions. Journal of Electrical Engineering & Technology. 2021; 16(4), 1879-1889.

[4] Sundaram BM, Manikandan BV, Kumar BP, Winston DP. Combination of novel converter topology and improved MPPT algorithm for harnessing maximum power from grid connected solar PV systems. Journal of Electrical Engineering & Technology. 2019; 14, 733-746.

[5] Padmavathi N, Chilambuchelvan A, Shanker NR. Maximum power point tracking during partial shading effect in PV system using machine learning regression controller. Journal of Electrical Engineering & Technology. 2021; 16, 737-748.

[6] Kumari N, Kumar SS, Laxmi V. Design of an efficient bipolar converter with fast MPPT algorithm for DC nanogrid application. International Journal of Circuit Theory and Applications. 2021; 49(9), 2812-2839.

[7] Thankakan R, Samuel Nadar ER. Investigation of the double input power converter with N stages of voltage multiplier using PSO-based MPPT technique for the thermoelectric energy harvesting system. International Journal of Circuit Theory and Applications. 2020; 48(3), 435-448.

[8] Kofinas P, Dounis AI, Papadakis G, Assimakopoulos MN. An Intelligent MPPT controller based on direct neural control for partially shaded PV system. Energy and Buildings. 2015; 90, 51-64.

[9] Kumar R, Khandelwal S, Upadhyay P, Pulipaka S. Global maximum power point tracking using variable sampling time and pv curve region shifting technique along with incremental conductance for partially shaded photovoltaic systems. Solar Energy. 2019; 189, 151-178.

[10] Bouarroudj N, Benlahbib B, Houam Y, Sedraoui M, Batlle VF, Abdelkrim T, et al. Fuzzy based incremental conductance algorithm stabilized by an optimal integrator for a photovoltaic system under varying operating conditions. Energy Sources, Part A: Recovery, Utilization, and Environmental Effects. 2021; 1-26.

[11] Nasir A, Rasool I, Sibtain D, Kamran R. Adaptive Fractional Order PID Controller Based MPPT for PV Connected Grid System Under Changing Weather Conditions. Journal of Electrical Engineering & Technology. 2021; 16(5), 2599-2610.

[12] Jiang M, Ghahremani M, Dadfar S, Chi H, Abdallah YN, Furukawa N. A novel combinatorial hybrid SFL–PS algorithm based neural network with perturb and observe for the MPPT controller of a hybrid PV-storage system. Control Engineering Practice. 2021; 114, 104880.

[13] Hamdi H, Regaya C B, Zaafouri A. Real-time study of a photovoltaic system with boost converter using the PSO-RBF neural network algorithms in a MyRio controller. Solar energy. 2019; 183, 1-16.

[14] Saidi AS, Salah CB, Errachdi A, Azeem MF, Bhutto JK, Ijyas VT. A novel approach in stand-alone photovoltaic system using MPPT controllers & NNE. Ain Shams Engineering Journal. 2021; 12(2), 1973-1984.

[15] Fathi M, Parian JA. Intelligent MPPT for photovoltaic panels using a novel fuzzy logic and artificial neural networks based on evolutionary algorithms. Energy Reports. 2021; 7, 1338-1348.

[16] Yılmaz M, Çorapsız, MF. Artificial Neural Network based MPPT Algorithm with Boost Converter topology for Stand-Alone PV System. Erzincan University Journal of Science and Technology. 2022; 15(1), 242-257.

[17] Yılmaz M, Kaleli A, Çorapsız MF. Machine learning based dynamic super twisting sliding mode controller for increase speed and accuracy of MPPT using real-time data under PSCs. Renewable Energy. 2023; 219, 119470.

[18] Ghazi GA, Hasanien HM, Al-Ammar EA, Turky RA, Ko W, Park S, Choi HJ. African vulture optimization algorithm-based PI controllers for performance enhancement of hybrid renewable-energy systems. Sustainability. 2022; 14(13), 8172.

[19] Houam Y, Terki A, Bouarroudj N. An efficient metaheuristic technique to control the maximum power point of a partially shaded photovoltaic system using crow search algorithm (CSA). Journal of Electrical Engineering & Technology. 2021; 16, 381-402.
[20] Aygül K, Cikan M, Demirdelen T, Tumay M. Butterfly optimization algorithm based maximum power point tracking of photovoltaic systems under partial shading condition. Energy Sources, Part A: Recovery, Utilization, and Environmental Effects. 2023; 45(3), 8337-8355.
[21] Tao H, Ghahremani M, Ahmed FW, Jing W, Nazir MS, Ohshima K. A novel MPPT controller in PV systems with hybrid whale optimization-PS algorithm based ANFIS under different conditions. Control Engineering Practice. 2021; 112, 104809.
[22] Pervez I, Shams I, Mekhilef S, Sarwar A, Tariq M, Alamri B. Most valuable player algorithm based maximum power point tracking for a partially shaded PV generation system. IEEE Transactions on Sustainable Energy. 2021; 12(4), 1876-1890.
[23] Fares D, Fathi M, Shams I, Mekhilef S. A novel global MPPT technique based on squirrel search algorithm for PV module under partial shading conditions. Energy Conversion and Management. 2021; 230, 113773.
[24] Mohammadinodoushan M, Abbassi R, Jerbi H, Ahmed FW, Rezvani A. A new MPPT design using variable step size perturb and observe method for PV system under partially shaded conditions by modified shuffled frog leaping algorithm-SMC controller. Sustainable Energy Technologies and Assessments. 2021; 45, 101056.
[25] Aldosary A, Ali ZM, Alhaider MM, Ghahremani M, Dadfar S, Suzuki K. A modified shuffled frog algorithm to improve MPPT controller in PV System with storage batteries under variable atmospheric conditions. Control Engineering Practice. 2021; 112, 104831.
[26] Eltamaly AM, Al-Saud MS, Abokhalil AG. A novel bat algorithm strategy for maximum power point tracker of photovoltaic energy systems under dynamic partial shading. IEEE Access. 2020; 8, 10048-10060.
[27] Mansoor M, Mirza AF, Ling Q. Harris hawk optimization-based MPPT control for PV systems under partial shading conditions. Journal of Cleaner Production. 2020; 274, 122857.
[28] Zafar MH, Khan NM, Mirza AF, Mansoor M, Akhtar N, Qadir MU, ... & Moosavi, et al. A novel meta-heuristic optimization algorithm based MPPT control technique for PV systems under complex partial shading condition. Sustainable Energy Technologies and Assessments. 2021; 47, 101367.
[29] Basha CH, Murali M. A new design of transformerless, non-isolated, high step-up DC-DC converter with hybrid fuzzy logic MPPT controller. International Journal of Circuit Theory and Applications. 2022; 50(1), 272-297.
[30] Kumar N, Hussain I, Singh B, Panigrahi BK. Rapid MPPT for uniformly and partial shaded PV system by using JayaDE algorithm in highly fluctuating atmospheric conditions. IEEE Transactions on Industrial Informatics. 2017; 13(5), 2406-2416.
[31] Alshareef M, Lin Z, Ma M, Cao W. Accelerated particle swarm optimization for photovoltaic maximum power point tracking under partial shading conditions. Energies. 2019; 12(4), 623.
[32] Bounabi M, Kaced K, Ait-Cheikh MS, Larbes C, Ramzan N. Modelling and performance analysis of different multilevel inverter topologies using PSO-MPPT technique for grid connected photovoltaic systems. Journal of Renewable and Sustainable Energy. 2018; 10(4).
[33] Eltamaly AM, Farh HM, Abokhalil AG. A novel PSO strategy for improving dynamic change partial shading photovoltaic maximum power point tracker. Energy sources, part a: recovery, utilization, and environmental effects. 2020; 1-15.
[34] Kamarzaman NA, Tan CW. A comprehensive review of maximum power point tracking algorithms for photovoltaic systems. Renewable and Sustainable Energy Reviews. 2014; 37, 585-598.
[35] Pal RS, Mukherjee V. Metaheuristic based comparative MPPT methods for photovoltaic technology under partial shading condition. Energy. 2020; 212, 118592.
[36] Al-Majidi SD, Abbod MF, Al-Raweshidy HS. A particle swarm optimisation-trained feedforward neural network for predicting the maximum power point of a photovoltaic array. Engineering Applications of Artificial Intelligence. 2020; 92, 103688.
[37] Reddy SS, Yammani C. A novel two step method to extract the parameters of the single diode model of Photovoltaic module using experimental Power–Voltage data. Optik. 2021; 248, 167977.
[38] Çevik K, Koçer H. A Soft Computing Application Based on Artificial Neural Networks Training by Particle Swarm Optimization. Süleyman Demirel University Journal of Natural and Applied Sciences. 2013; 17(2), 39-45.